ELSEVIER

Synthesis, characterization, and reactions of 6,13-disubstituted 2,3,9,10-tetrakis(trimethylsilyl)pentacene derivatives

Yu-Man Wang,[a,b,c] Nan-Yan Fu,[d] Siu-Hin Chan,[a,b,c] Hung-Kay Lee[a] and Henry N. C. Wong[a,b,c,*]

[a]*Department of Chemistry, The Chinese University of Hong Kong, Shatin, New Territories, Hong Kong SAR, China*
[b]*Centre of Novel Functional Molecules, The Chinese University of Hong Kong, Shatin, New Territories, Hong Kong SAR, China*
[c]*Central Laboratory of the Institute of Molecular Technology for Drug Discovery and Synthesis,[†]*
The Chinese University of Hong Kong, Shatin, New Territories, Hong Kong SAR, China
[d]*Department of Chemistry, Fuzhou University, Fuzhou, Fujian 350002, China*

Abstract—Pentacene has been actively studied as relevant materials in organic field-effect transistors (OFETs) and organic light-emitting diodes (OLEDs). However, the low solubility and low stability of pentacene in common organic solvents have hindered its applications. When exposed to light or at high concentration, pentacene is found to dimerize easily. Many research groups are currently working on the design and synthesis of novel substituted pentacenes, but few of them systematically reported physical properties such as molecular spectroscopy and electronic properties, which might elucidate the influence of substituents on HOMO–LUMO gaps. Furthermore, the reactive nature of the central ring in pentacenes makes pentacenes good dienes for Diels–Alder reactions. In this paper, a series of soluble 6,13-disubstituted 2,3,9,10-tetrakis(trimethylsilyl)pentacenes were synthesized and characterized. Their reactions, structures, and physical properties were also studied. In addition, bulky *o*-carboranyl substituted pentacene derivative **15** and 6-chloro-2,3,9,10-tetrakis(trimethylsilyl)pentacene (**16**) were synthesized for the first time. Compound **16** possesses the largest dihedral angle (7.7° with two adjacent benzene rings) and shows a wave structure. Diels–Alder reactions with acceptable efficiency were carried out between **16** and various dienophiles.
© 2007 Elsevier Ltd. All rights reserved.

1. Introduction

Over the past decades, organic semiconductors have been studied extensively in the fabrication of organic field-effect transistors (OFETs).[1–9] Because of its high mobility for hole transport pentacene was studied as a promising candidate, as a p-type semiconductor. It has also found use in organic light-emitting diodes (OLEDs),[10] where the typically high florescence efficiency of this aromatic compound makes it an ideal red emitter. However, the low solubility and low stability have hindered widespread use of pentacene in device fabrication because vacuum deposition method is expensive and spin-casting method needs good solubility of the pentacene. On the other hand, herringbone packing in the solid state also influences the performance of devices based on organic active layer materials.[11,12] In particular, the amount of π-orbital overlap is expected to have a strong influence on field-effect mobility. One approach to improve pentacene-based device performance is to modify the pentacene molecule by means of suitable substituents. Elegant works of Anthony and co-workers revealed that attachment of

trialkylsilylethynyl moieties to the central ring of pentacene could increase its solubility and stability.[12–16] An empirical model was built accordingly to predict the solid-state order of functionalized pentacenes.[4] The introduction of substituents in the 2, 3, 9, and 10 positions of pentacene also affects the overall properties of pentacene due to various electronic and geometric parameters of substituents.[11] As reported by Neckers, ethynyl moieties on the terminal rings were used to tune the electronic properties of pentacene derivatives, leading to the lowest HOMO–LUMO gap of 1.693 eV.[11] Wong and co-workers reported the soluble 2,3,9,10-tetrakis(trimethylsilyl)pentacene (**14**) and studied its electrochemical properties as well as Diels–Alder reactivities.[1] Hopf and co-workers synthesized a diether pentacene derivative, but the solubility of this pentacene derivative in common organic solvents was lower than those of the tetracene analogs.[17]

Herein, we report the successful synthesis and physical properties of a series of 6,13-disubstituted 2,3,9,10-tetrakis(trimethylsilyl)pentacene derivatives **2–13** possessing good solubility and stability. Furthermore, computational method was also used to mimic different substituted pentacene derivatives, and helped us to elucidate the influence of substituents that may offer a theoretical basis toward the design of

potentially high-performance pentacene materials. In addition, a bulky *o*-carboranyl substituted pentacene derivative **15** was synthesized and fully characterized by spectroscopic analysis. An inter-planar distance of 10.46 Å was found, which is by far the largest value known today. This result provides an insight into the prevention of dimerization of reactive pentacene molecules, and as a result widens the chemistry of carboranes and pentacenes. 6-Chloro-2,3,9,10-tetrakis(trimethylsilyl)pentacene (**16**) was firstly synthesized and elucidated to contain a non-planar wave crystal structure. Diels–Alder reactions were also studied between **16** and different dienophiles.

2. Results and discussion

As illustrated in Scheme 1, the introduction of substituents to the central ring of pentacene was carried out with 65–95% yields by reactions between 2,3,9,10-tetrakis(trimethylsilyl)pentacene-6,13-dione (**1**)[18] and the corresponding Grignard or organolithium reagents. 6,13-Diethynyl substituted pentacene derivatives **2–6** were typically prepared after reduction of the resulting diols with tin(II) chloride saturated with 10% HCl. The resulting blue products are all stable both as solids and in solutions, even when exposed to light and air. Substituted aryllithium and thienyllithium were generated by lithium–halogen or lithium–hydrogen exchange of the corresponding arylbromide or thiophene, respectively, by treatment with *n*BuLi. Introduction of the substituents proceeded smoothly upon addition of the freshly prepared aryllithium or thienyllithium **1**, and subsequent reduction as previously described provided **7–13**. Again, compounds **7–13** are stable both in solutions and in solid states, but they were found to undergo oxidation easily when exposed to light and air.

The crystal structure of compound **9** is shown in Figure 1.[19] As can be seen, the inter-planar distance is 5.44 Å (compared with 6.27 Å for unsubstituted pentacene[20,21]). Use of

more complicated functionalities on the pentacene skeleton could control the molecular orientation, therefore yielding materials that would show good π-overlap in the solid state. *p*-Methoxyphenyl substituted pentacene derivative **9** exhibits a nearly planar structure with a dihedral angle of 1.1° for the two adjacent benzene rings with C–H···π-stacking in the molecular arrangement.

Pentacene easily undergoes photo-oxidation when it is exposed to light and oxygen due to the high reactivity of the pentacene molecule.[1,4] The photochemical stability of compound **8** was assessed. Thus, pentacene **8** was dissolved in dichloromethane at room temperature and transferred to a UV quartz cell bubbled with N_2. The mixture was then allowed to expose to light and air. The measurement was carried out at different times (Fig. 2). Along with the exposition to light and oxygen, it can be seen that the intensity of the peak at 325 nm (π–π* transition) decreased slowly, and a new peak formed at 262 nm. After 100 min, the process was at equilibrium with $t_{1/2}=30$ min. The phenomenon is consistent with the disruption of conjugation expected as a result of the formation of an *endo* peroxide across the central ring of the pentacene unit.

The UV–vis spectra of 2,3,9,10-tetrakis(trimethylsilyl)pentacene (**14**)[1] and its derivatives **2**, **7**, and **12** are shown in Figure 3. All measurements were carried out in dichloromethane at room temperature without light and oxygen. It can be seen clearly that all three substituted pentacenes **2**, **7**, and **12** display a large red-shift as compared to **14** without substituents at 6 and 13 positions. It indicates the effect of a stronger π conjugation of these 6,13-disubstituted molecules. Amongst the ethynyl, aryl, and thienyl substituted pentacenes, ethynylated pentacene **2** shows the largest red-shift to the longer wavelength, which indicates that the ethynyl group is a better conductor of electronic effects.

Electron-withdrawing groups and electron-donating groups on the aryl substituents may also show influence on the
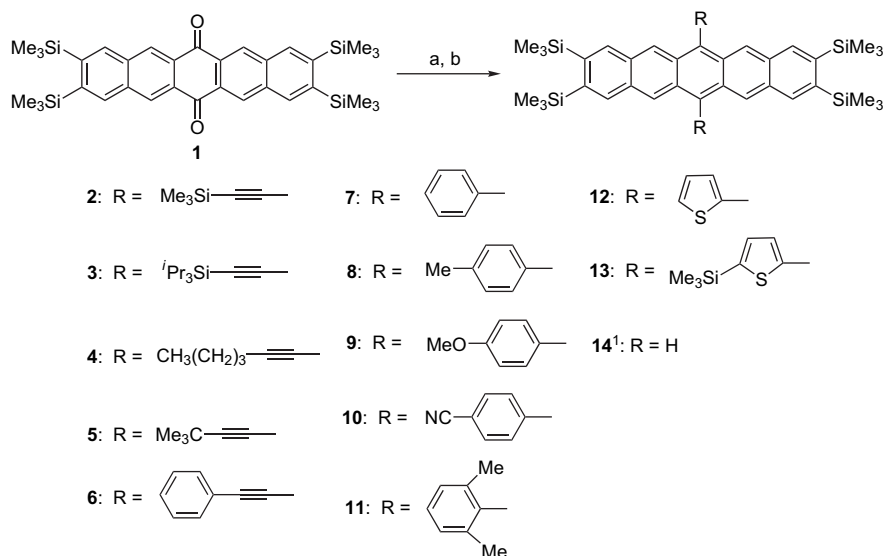
Scheme 1. Reagents and conditions: **2–6**: Compounds (a) R–H, Mg, EtBr, THF, reflux, 3 h. (b) Satd SnCl₂/10% HCl, THF, reflux, 1 h. Compounds **7–11**: (a) R–Br, *n*BuLi, THF, –78 °C, 3 h. (b) Satd SnCl₂/10% HCl, THF, reflux, 1 h. Compounds **12** and **13**: (a) R–H, *n*BuLi, THF, –78 °C, 3 h. (b) Satd SnCl₂/10% HCl, THF, reflux, 1 h.
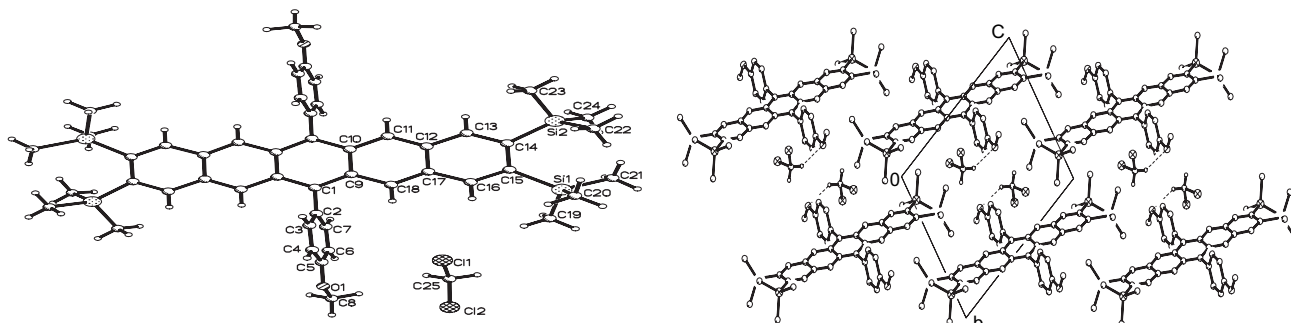
Figure 1. Crystallographic order of compound **9**. Left: single molecule; right: viewed along the *a*-axis.
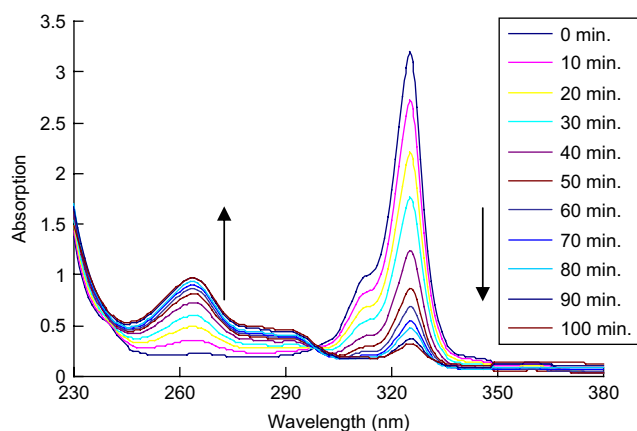

Figure 2. Photochemistry of compound **8** in the presence of light and air at different periods of time.
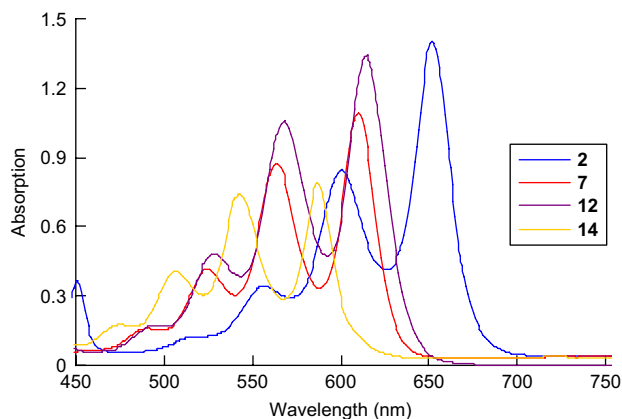

Figure 3. UV–vis spectra of **14** and its derivatives **2**, **7**, and **12**.

Figure 4. UV–vis spectra of different aryl substituted pentacene derivatives **7**, **9**, and **10**.

table, the maxima of all these pentacenes are around 580–670 nm, and the absorption maxima of these compounds are red-shifted in the order of **14** without substitutions at 6 and 13 positions<aryl substituted pentacenes **7–11** and thienyl substituted pentacenes **12** and **13**<ethynylated pentacenes **2–6**. It therefore reveals that substituents in 6 and 13 positions of pentacene, especially the ethynyl groups, could greatly lower the HOMO–LUMO gap and stabilize the pentacene molecules.

Fluorescence spectra of compounds **2–14** were also measured in the absence of light and oxygen. The fluorescence data are also listed in Table 1. As a result, the emission of pentacene **14** is largely blue-shifted relative to compounds **2–13**. The data are consistent with the absorption results. Figure 5 shows the normalized absorption and fluorescence spectra of compound **8** in dichloromethane. The small red-shift of 20 nm for compound **8** suggests that molecular rearrangement took place due to the photoexcitation of the molecule.

Cyclic voltammetry (CV) of compounds **2–13** (Compound **14** was reported by Wong and co-workers with $E_{ox} = +0.25$ eV, $E_{red} = -1.81$ eV, and $\Delta E_{HOMO-LUMO} = 2.06$ eV[1]) were measured in dichloromethane containing $^{n}Bu_4NPF_6$ (0.1 M) at room temperature without light and oxygen, and ferrocene/ferrocenium (Fc/Fc$^+$) was used as the standard redox system. All compounds show one reversible oxidation and one reversible reduction and $\Delta E_{HOMO-LUMO}$ was calculated (Table 1). From these values, the HOMO and LUMO energies change greatly from 6,13-disubstituted pentacenes **2–13** to pentacene **14**. It is clear that substituents on the

absorption of pentacene molecules. Thus, UV–vis spectra of different aryl substituted pentacene derivatives **7**, **9**, and **10** with different concentrations in dichloromethane were carried out. The results are shown in Figure 4. As can be seen, the absorption maxima of all three pentacenes are nearly identical around 609 nm. It can be concluded that the electron-donating and electron-withdrawing groups on the aryl groups lead to a small influence on the overall absorptions of pentacene derivatives.

In summary, data of absorption spectra of all disubstituted pentacene derivatives are listed in Table 1. As shown in the
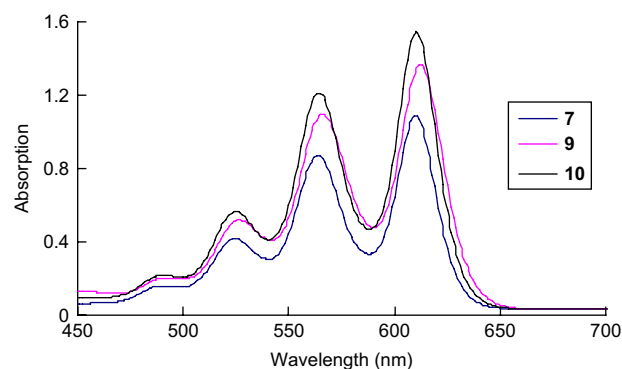
Table 1. Synthetic yields and spectroscopic and electrochemical data for compounds **2–14**

Compound	Yield (%)	λ_{max} (abs) (nm)	λ_{max} (em) (nm)	E_{ox} (eV)	E_{red} (eV)	$\Delta E_{HOMO-LUMO}$ (eV)
2	95	650	669	0.315	−1.415	1.73
3	80	652	662	0.380	−1.456	1.84
4	87	641	672	0.325	−1.485	1.81
5	85	643	655	0.266	−1.603	1.87
6	91	665	682	0.325	−1.765	2.09
7	76	609	627	0.265	−1.755	2.02
8	80	610	630	0.256	−1.750	2.01
9	65	611	629	0.265	−1.755	2.02
10	84	609	630	0.355	−1.695	2.05
11	70	610	632	0.267	−1.843	2.11
12	76	613	634	0.295	−1.615	1.91
13	80	617	635	0.345	−1.585	1.93
14	80	585	600	0.254	−1.806	2.06[1]
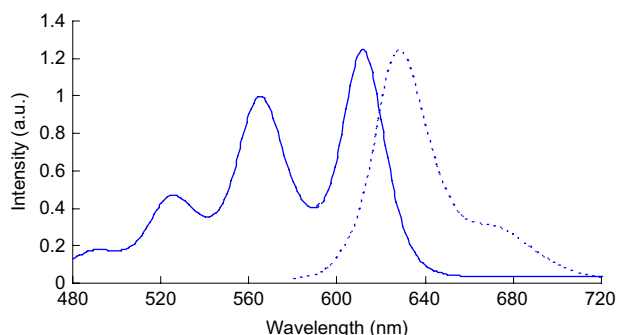
Figure 5. Normalized absorption (solid line) and fluorescence (dashed line) spectra of compound **8** in dichloromethane.

central rings of pentacene could tune or even alter the electronic properties of these pentacene derivatives. It can also be concluded that compounds with ethynyl groups possess the lowest $\Delta E_{HOMO-LUMO}$ when compared to other substituted pentacenes. Due to the high oxidation potential, the substituted pentacenes **2–13** are less prone to be oxidized than pentacene **14**. Figure 6 shows the cyclic voltammogram of compound **8**, and the oxidation and reduction processes are chemically and electrochemically reversible.

Acenes consisting of linearly fused benzene rings have also attracted wide interest from theoretical chemists. The electronic structures, stabilities, aromaticity, and most importantly the band gaps or HOMO–LUMO gaps of such oligoacenes or polyacenes are still the subject of controversy.[22–25] DFT methods have been used as a popular and reliable tool to optimize the geometry and analyze the
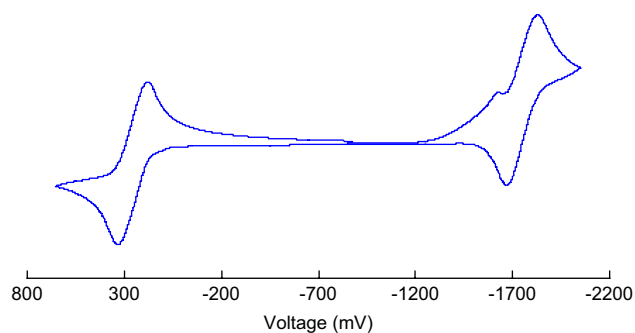
Figure 6. Cyclic voltammogram of compound **8**.

electronic structure. Based on geometry optimization, the HOMO–LUMO gaps of pentacene and its derivatives were calculated at B3LYP/6-31G(d) level. The calculation results are shown in Table 2. The geometry optimization results show that linear pentacene and its derivatives possess a planar backbone. Comparison of the calculated HOMO–LUMO gaps of unsubstituted pentacene (2.2110 eV), trimethylsilylethynyl group at 1, 2, 5, and 6 positions of pentacene reduced the HOMO–LUMO gap by 0.0460, 0.0482, 0.1177, and 0.1512 eV, respectively. This indicates that the substituents on the central ring demonstrate more pronounced influence than those on the side rings. The influence of trimethylsilylethynyl groups at different ring positions was found to be very similar.
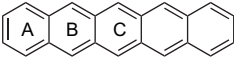
Nucleus-independent chemical shifts (NICS) were used to characterize the aromaticity of polyacenes by Schleyer.[26–28] NICS(0) is calculated at the ring center and NICS(1) is calculated at 1 Å above the ring. Aromatic rings are usually characterized by negative values and the more negative the NICS value the more aromatic would be the compound. Schleyer found that in acenes the inner rings demonstrate more negative NICS values than those in the side rings. Diels–Alder addition of acetylene to acenes is used as a model to determine the relationship between aromatic stabilization and reactivity. The inner rings with more negative NICS values have higher reactivity towards acetylene, and are consistent with the observed experimental results.[26–28] The NICS value of benzene and pentacene calculated by Schleyer are shown in Table 3. These values can also be used to predict the influence of substituents on pentacene at different positions.

The trimethylsilylethynyl groups of 6,13-bis(trimethylsilylethynyl)pentacene were found to possess a HOMO–LUMO gap of 0.3094 eV that is twice the amount as that of 6-trimethylethynylpentacene. This shows that the influence of substituent on HOMO–LUMO gap is likely linear. The computational results point to the fact that four trimethylsilyl groups at 2, 3, 9, and 10 positions only reduce the HOMO–LUMO gap by 0.0047 eV. Therefore, the introduction of four trimethylsilyl groups on the side rings of pentacene actually only increases the solubility dramatically, but without changing the HOMO–LUMO gap significantly. 6-Phenyl group substitution reduces the HOMO–LUMO gap by 0.0204 eV, which is much lower than that for the trimethylsilylethynyl group, indicating no conjugation between

Table 2. Calculated HOMO–LUMO gap of pentacene derivatives at B3LYP/6-31G(d) level

Compound R	LUMO (au)	HOMO (au)	HOMO–LUMO gap			
			(au)	(kcal/mol)	(eV)	(nm)
H	–0.08773	–0.16898	0.081250	50.984	2.2110	562.26
6-Me$_3$SiC≡C–	–0.09379	–0.16944	0.075650	47.470	2.0586	603.88
5-Me$_3$SiC≡C–	–0.09281	–0.16970	0.076890	48.248	2.0923	594.15
1-Me$_3$SiC≡C–	–0.09079	–0.17035	0.079560	49.924	2.1650	574.21
2-Me$_3$SiC≡C–	–0.09217	–0.17165	0.079480	49.874	2.1628	574.78
6,13-Bis(Me$_3$SiC≡C)–	–0.09946	–0.16934	0.069880	43.850	1.9016	653.75
6-Ph	–0.08654	–0.16704	0.080500	50.514	2.1906	567.50
6-Cl	–0.09457	–0.17410	0.079530	49.905	2.1642	574.42
14	–0.08904	–0.17012	0.081080	50.878	2.2063	563.44
16	–0.09487	–0.17432	0.079450	49.855	2.1620	575.00

Table 3. NICS data of pentacene[28]

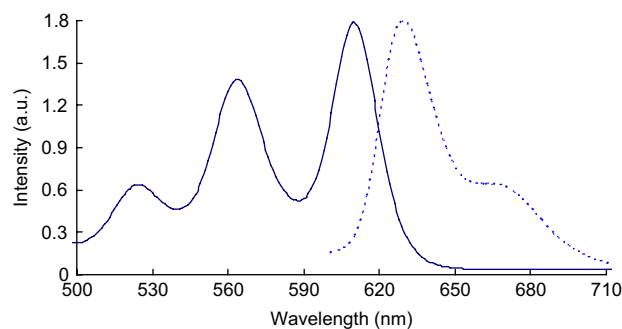| Acenes		NICS(0)	NICS(1)
(benzene ring)		–8.8	–10.6
(A B C pentacene)	A	–5.8	–8.5
	B	–10.7	–12.6
	C	–12.2	–13.9

the phenyl ring and the pentacene backbone. The phenyl ring is perpendicular to the pentacene backbone due to H–H repulsion as shown by geometry optimization and X-ray results. It can be further confirmed by our experimental results that substituents on the phenyl ring have almost no influence on the HOMO–LUMO gap. We therefore predict that the value of the HOMO–LUMO gap of 6,13-bis(trimethylsilylethynyl)-2,3,9,10-tetrakis(trimethylsilyl)pentacene (**2**) is lower than that of 2,3,9,10-tetrakis(trimethylsilyl)pentacene (**14**) by around 0.3 eV. The experimental data for **2** and **14** are 1.73 and 2.06 eV, respectively, nonetheless confirming our prediction.
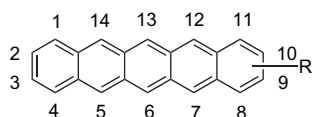
Bulky 6,13-di-o-carboranyl substituted pentacene derivative **15** was firstly synthesized and has provided the insight into

the prevention of dimerization of these reactive linearly extended benzenoid pentacene molecules. Compound **15** was synthesized at –50 °C with 11% yield as a purple-red solid (Scheme 2). Figure 7 shows the absorption (λ_{max}=609 nm) and emission (λ_{max}=632 nm) spectra of **15** in dichloromethane. Figure 8 shows the cyclic voltammogram of compound **15** with $\Delta E_{HOMO-LUMO}$=2.067 eV. Compound **15** shows one reversible oxidation and three reductions. These oxidation and reduction potentials are +0.211, –0.947, –1.856, and –2.063 eV, respectively. In the reduction regions, the LUMO of o-carborane is located at –0.947 and –2.063 eV. Figure 9 shows the crystal structure of compound **15**.[29] Due to substitution of large o-carboranyl groups, the inter-planar distance of compound **15** was 10.46 Å, which is the largest value known today.

Figure 7. Absorption and emission spectra of compound **15**.
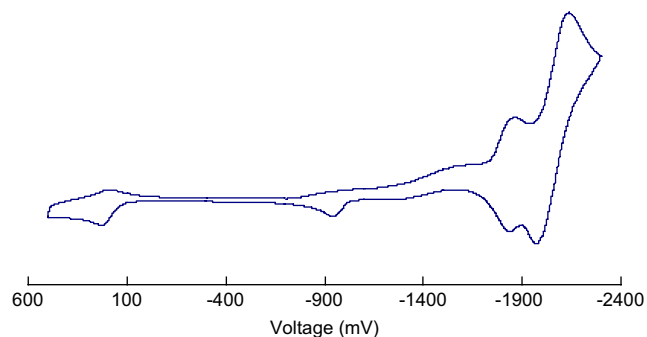

Scheme 2. Reagents and conditions: (a) R–H, R–Br, ^{n}BuLi, ether/toluene=2:1, –50 °C, 3 h. (b) Satd SnCl$_2$/10% HCl, THF, reflux, 1 h, 11%.

Figure 8. Cyclic voltammogram of compound **15**.

Figure 10. Absorption and emission spectra of compound **16**.

Pentacenequinone **1** was reduced by LiAlH$_4$ at 0 °C, and subsequent reaction of the corresponding hydroxyl group with MsCl at room temperature led to a rapid color change of the reaction mixture from yellow to blue. After a rapid flash column chromatography performed with hexanes as an eluent in the absence of light and oxygen, 6-chloro-2,3,9,10-tetrakis(trimethylsilyl)pentacene (**16**) was obtained in 46% yield as a purple-red solid (Scheme 3).

The absorption and emission spectra (Fig. 10) of compound **16** were measured in dichloromethane under the condition without light and oxygen. The absorption (λ_{max}=610 nm) is 25 nm red-shifted as compared to 2,3,9,10-tetrakis(trimethylsilyl)pentacene (**14**). In addition, a red-shift of 33 nm in the emission energy (λ_{max}=633 nm) is observed compared to **14**. Cyclic voltammetry performed on **16** in
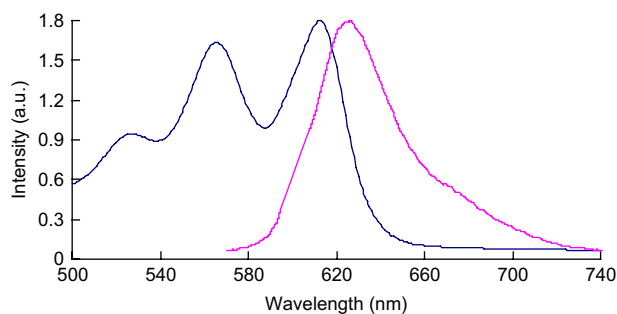
dichloromethane shows a fully reversible oxidation and reduction at +0.295 and −1.712 eV with $\Delta E_{HOMO-LUMO}$= 2.007 eV (Fig. 11). The value from cyclic voltammetry corresponds well with the calculated HOMO–LUMO gap, which is 2.162 eV.

Compound **16** was found to be relatively more stable than 2,3,9,10-tetrakis(trimethylsilyl)pentacene (**14**), which is able to dimerize at high concentration even in darkness.[1] 6-Chloro-2,3,9,10-tetrakis(trimethylsilyl)pentacene (**16**) can be kept for several weeks under darkness and does not even decompose significantly after being heated at 150 °C for 2 days. However, the color of a solution of **16** under sunlight and air can only persist for less than 15 min with the formation of 2,3,9,10-tetrakis(trimethylsilyl)-6,13-dihydropentacene-6,13-dione (**1**), presumably via **22** as the intermediate (Scheme 4).
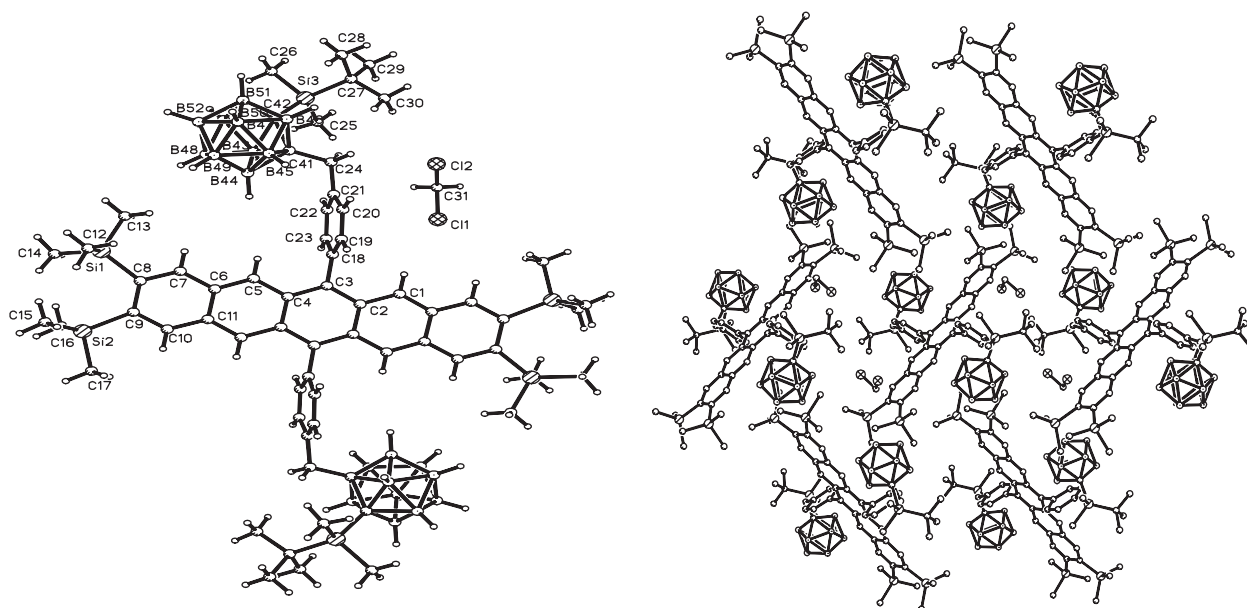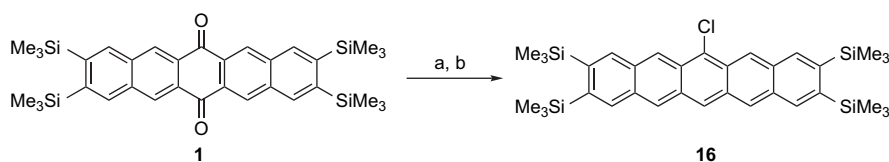

Figure 9. Crystallographic order of compound **15**. Left: single molecule; right: viewed along the *a*-axis.

Scheme 3. Reagents and conditions: (a) LAH, THF, 0 °C, 15 min. (b) MsCl, TEA, DMAP, CH$_2$Cl$_2$, rt, 1 h, 46% (two steps).
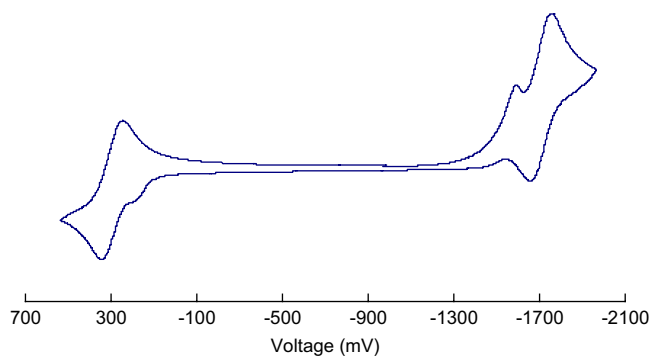
**Figure 11**. Cyclic voltammogram of compound **16**.

It is clear that the peroxide formation rate of **16** is faster than those of the aryl substituted pentacene derivatives as mentioned above. Due to the fact that peroxide formation would likely involve a radical species, we also measured both the EPR properties of **16** in the absence and the presence of oxygen. We found that, in the absence of oxygen, compound **16** did not show an EPR signal. On the other hand, when a solution of **16** was allowed to come into contact with atmospheric oxygen, an EPR signal centered at $g=2.00$ was detected (Fig. 12). We also assume that the origin of the

EPR signal is due to the presence of radical cation of **16** as depicted in Scheme 5.

Figure 13 shows the crystal structure of compound **16**.[30] In the literature, all pentacenes have nearly planar structures. However, X-ray structure of **16** (with inter-planar distance of 3.865 Å) shows the largest dihedral angle (7.7° with two adjacent benzene rings) and possesses a wave structure. This might be due to the strong electron-withdrawing chloro group. Compound **16** also presents a one-dimensional π-stacking.

Diels–Alder reactions between 6-chloro-2,3,9,10-tetrakis-(trimethylsilyl)pentacene (**16**) and different dienophiles were also carried out. The reactions are not as complicated as those of 2,3,9,10-tetrakis(trimethylsilyl)pentacene (**14**).[1] The reactions were easy to operate due to the more stable nature of **16** with also its modest reactivity (Scheme 6).

In conclusion, we have synthesized a series of soluble and stable pentacenes. Their physical properties and reactions were fully studied by virtue of their solubility in organic solvents. In addition, bulky o-carboranyl substituted pentacene derivative was realized, which has provided an insight into the prevention of dimerization of these reactive pentacene
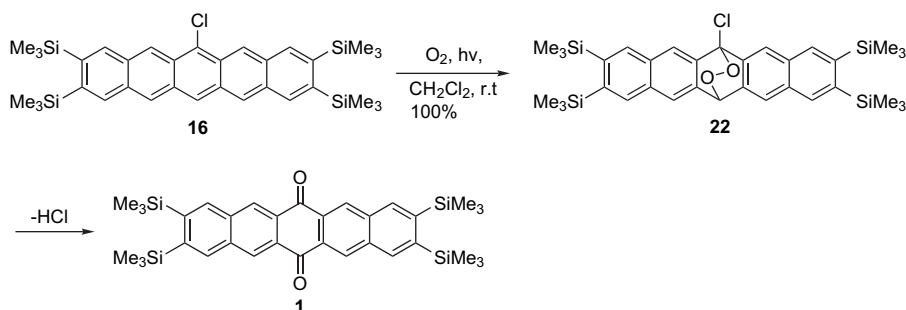
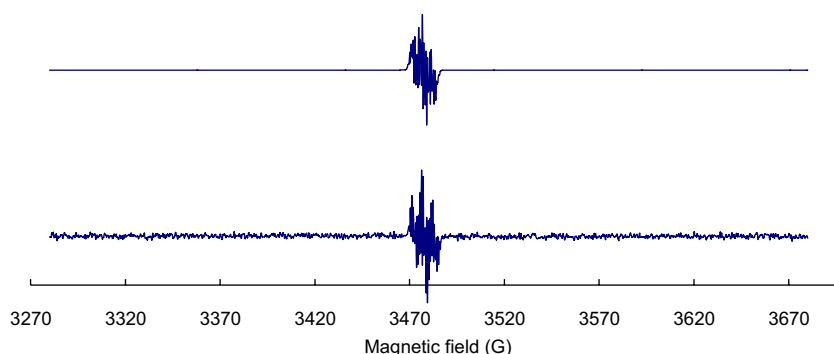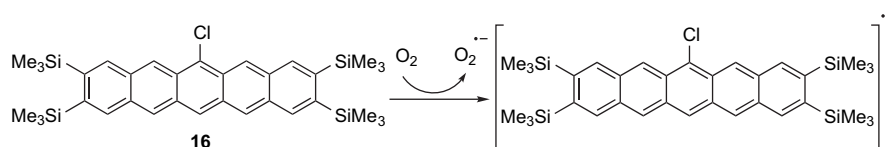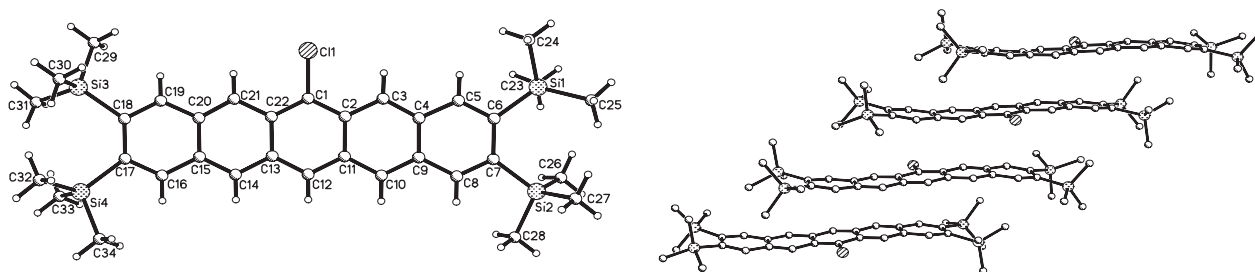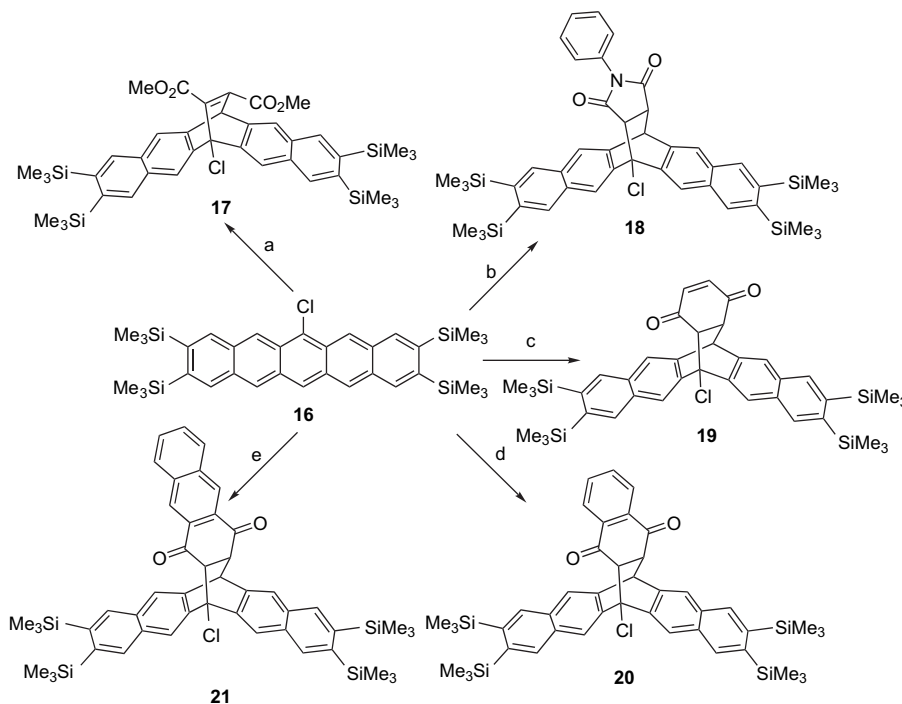**Scheme 4**. Oxidation of compound **16**.

Figure 12. EPR spectrum of compound **16** in dichloromethane at 298 K (bottom) and its computer simulation (top).

Scheme 5. Radical transformation of compound **16** with O$_2$.

Figure 13. Crystallographic order of compound **16**. Left: single molecule; right: viewed along the *a*-axis.

Scheme 6. Reagents and conditions: (a) DMAD, CH₂Cl₂, rt, 2 days, 36%. (b) *N*-Phenyl maleimide, CH₂Cl₂, rt, 12 h, 86%. (c) *p*-Benzoquinone, CH₂Cl₂, rt, 12 h, 80%. (d) Naphthaquinone, CH₂Cl₂, rt, 12 h, 48%. (e) Anthraquinone, CH₂Cl₂, rt, 12 h, 43%.

molecules. 6-Chloro-2,3,9,10-tetrakis(trimethylsilyl)penta-cene (**16**) was synthesized, and found to show a non-planar wave structure due presumably to the strong electron-with-drawing chloro group.

3. Experimental

3.1. General information

All reagents and solvents were reagent grade. Further puri-fication and drying by standard methods were employed when necessary. The plates used for thin-layer chromato-graphy (TLC) were E. Merck silica gel 60F₂₅₄ (0.24 nm thickness) precoated on aluminum plates, and then visual-ized under both long (365 nm) and short (254 nm) UV light. Compounds on TLC plates were visualized with a spray of 5% dodecamolybdophosphoric acid in ethanol and with sub-sequent heating. Column chromatography was performed using E. Merck silica gel (230–400 mesh).

Melting points were measured on a Reichert Microscope ap-paratus and were uncorrected. NMR spectra were recorded on a Bruker DPX-300 spectrometer (300.13 MHz for ¹H and 75.47 MHz for ¹³C). All NMR measurements were car-ried out at 300 K in deuterated chloroform unless otherwise stated. Mass spectra (ESI and HRMS) were obtained with a Thermofinnigan MAT95XL spectrometer and determined at an ionized voltage of 70 eV unless otherwise stated. Rel-evant data are tabulated as *m/z*. UV–visible spectra were ob-tained on a CARY 5E UV-vis-NIR spectrophotometer (in the range of 200–800 nm) using 1-cm quartz cells. Fluorescence was recorded from 500 to 800 nm on a Hitachi F4500 fluo-rescence spectrophotometer with excitation and emission slit widths set at 1.0 nm. CV measurements were carried out at 25 °C under N₂ using a BAS CV-50W voltammetric analyzer. A three-electrode system, which consisted of a plat-inum ball working electrode, a silver reference electrode, and a platinum foil auxiliary electrode was used with [Bu₄N]⁺[PF₆]⁻ as the supporting electrolyte. All redox po-tentials are referenced to the ferrocenium/ferrocene redox

couple as recommended by the IUPAC. Elemental analyses were performed at Shanghai Institute of Organic Chemistry, The Chinese Academy of Sciences, China.

3.1.1. General procedure for the preparation of pentacene derivatives 2–6.

3.1.1.1. 6,13-Bis(trimethylsilylethynyl)-2,3,9,10-tetrakis(trimethylsilyl)pentacene (2). To a suspension of Mg (82 mg, 3.4 mmol) in THF (10 mL) in a flame-dried three-necked round-bottomed flask, ethyl bromide (0.25 mL, 3.4 mmol) was added dropwise under N_2. After refluxing for 1 h, the reaction mixture was cooled to room temperature and trimethylsilyl acetylene (0.52 mL, 3.7 mmol) was added via a syringe. The reaction mixture was heated to reflux again for another 1 h and then cooled to room temperature. Pentacenequinone **1** (100 mg, 0.17 mmol) was added and the mixture was refluxed for a further 1 h. After cooling to room temperature, a solution of 10% aqueous HCl (5 mL) saturated with $SnCl_2$ was added carefully until the flask content no longer bubbled on addition of the $SnCl_2$ solution. The solution was then heated to reflux for 1 h before being allowed to cool. The mixture was filtered through a short pad of silica gel eluting with hexanes and the solvent was removed under reduced pressure. The resulting crude product was purified by column chromatography on silica gel (20 g, hexanes) to afford **2** (120 mg, 95%) as a deep blue solid: mp 311 °C (decomp.); ^{1}H NMR (CDCl$_3$) δ 0.50 (s, 36H), 0.57 (s, 18H), 8.31 (s, 4H), 9.11 (s, 4H); ^{13}C NMR (CDCl$_3$) δ 0.3, 1.9, 103.1, 110.5, 118.4, 125.9, 130.9, 131.1, 136.6, 141.9; MS m/z 758 (M$^+$), HRMS (ESI) Calcd for $C_{44}H_{62}Si_4$ (M$^+$): 758.3452. Found: 758.3453. Anal. Calcd for $C_{44}H_{62}Si_6$: C, 69.58; H, 8.23. Found: C, 69.75; H, 8.44.

3.1.1.2. 6,13-Bis(triisopropylsilylethynyl)-2,3,9,10-tetrakis(trimethylsilyl)pentacene (3). This was prepared from Mg (82 mg, 3.4 mmol), ethyl bromide (0.25 mL, 3.4 mmol), triisopropylsilyl acetylene (0.83 mL, 3.7 mmol), **1** (100 mg, 0.17 mmol), and 10% HCl (5 mL) saturated with $SnCl_2$ in THF (10 mL) in the same manner as described above, yielding **3** (126 mg, 80%) as a deep blue solid: mp 290 °C (decomp.); ^{1}H NMR (CDCl$_3$) δ 0.49 (s, 36H), 1.38 (s, 6H), 1.40 (s, 36H), 8.28 (s, 4H), 9.23 (s, 4H); ^{13}C NMR (CDCl$_3$) δ 1.7, 11.7, 18.9, 104.7, 107.1, 118.7, 126.1, 131.0, 131.1, 136.6, 141.8; MS m/z 926 (M$^+$), HRMS (ESI) Calcd for $C_{56}H_{86}Si_6$ (M$^+$): 926.5340. Found: 926.5329. Anal. Calcd for $C_{56}H_{86}Si_6$: C, 72.49; H, 9.34. Found: C, 72.59; H, 9.63.

3.1.1.3. 6,13-Dihexynyl-2,3,9,10-tetrakis(trimethylsilyl)pentacene (4). This was prepared from Mg (82 mg, 3.4 mmol), ethyl bromide (0.25 mL, 3.4 mmol), 1-hexyne (0.43 mL, 3.7 mmol), **1** (100 mg, 0.17 mmol), and 10% HCl (5 mL) saturated with $SnCl_2$ in THF (10 mL) in the same manner as described above, yielding **4** (107 mg, 87%) as a deep blue solid: mp 320 °C (decomp.); ^{1}H NMR (CDCl$_3$) δ 0.52 (s, 36H), 1.19 (t, J=7.2 Hz, 6H), 1.83–2.01 (m, 8H), 3.00 (t, J=6.9 Hz, 4H), 8.33 (s, 4H), 9.13 (s, 4H); ^{13}C NMR (CDCl$_3$) δ 2.0, 13.9, 20.4, 22.4, 31.2, 79.0, 105.4, 118.7, 125.9, 130.9, 131.0, 136.8, 141.3; MS m/z 726 (M$^+$), HRMS (ESI) Calcd for $C_{46}H_{62}Si_4$ (M$^+$): 726.3923. Found: 726.3929.

3.1.1.4. 6,13-Bis(3,3-dimethyl-1-butynyl)-2,3,9,10-tetrakis(trimethylsilyl)pentacene (5). This was prepared from Mg (82 mg, 3.4 mmol), ethyl bromide (0.25 mL, 3.4 mmol), 3,3-dimethyl-1-butyne (0.46 mL, 3.7 mmol), **1** (100 mg, 0.17 mmol), and 10% HCl (5 mL) saturated with $SnCl_2$ in THF (10 mL) in the same manner as described above, yielding **5** (105 mg, 85%) as a deep blue solid: mp 320 °C (decomp.); ^{1}H NMR (CDCl$_3$) δ 0.50 (s, 36H), 1.70 (s, 18H), 8.28 (s, 4H), 9.07 (s, 4H); ^{13}C NMR (CDCl$_3$) δ 1.9, 29.3, 31.4, 77.2, 113.6, 118.5, 125.5, 125.8, 130.8, 136.7, 141.3; MS m/z 726 (M$^+$), HRMS (ESI) Calcd for $C_{46}H_{62}Si_4$ (M$^+$): 726.3923. Found: 726.3927. Anal. Calcd for: $C_{46}H_{62}Si_4$: C, 75.96; H, 8.59. Found: C, 75.07; H, 8.90.

3.1.1.5. 6,13-Bis(phenylethynyl)-2,3,9,10-tetrakis(trimethylsilyl)pentacene (6). This was prepared from Mg (82 mg, 3.4 mmol), ethyl bromide (0.25 mL, 3.4 mmol), phenyl acetylene (0.41 mL, 3.7 mmol), **1** (100 mg, 0.17 mmol), and 10% HCl (5 mL) saturated with $SnCl_2$ in THF (10 mL) in the same manner as described above, yielding **6** (118 mg, 91%) as a blue-green solid: mp 326 °C (decomp.); ^{1}H NMR (CDCl$_3$) δ 0.51 (s, 36H), 7.51–7.60 (m, 4H), 7.96 (dd, J=8.1, 1.5 Hz, 4H), 8.34 (s, 4H), 9.21 (s, 4H); ^{13}C NMR (CDCl$_3$) δ 2.0, 87.9, 104.2, 118.5, 123.7, 125.9, 128.7, 128.8, 130.9, 131.1, 131.9, 136.6, 142.0; MS m/z 766 (M$^+$), HRMS (ESI) Calcd for $C_{50}H_{54}Si_4$ (M$^+$): 766.3297. Found: 766.3291.

3.1.2. General procedure for the preparation of pentacene derivatives 7–13.

3.1.2.1. 6,13-Diphenyl-2,3,9,10-tetrakis(trimethylsilyl)pentacene (7). To a solution of bromobenzene (0.36 mL, 3.4 mmol) in THF (10 mL) at −78 °C was added ^{n}BuLi (2.1 mL, 3.4 mmol) dropwise. After stirring for 1 h at −78 °C, phenyllithium was transferred dropwise to the solution of **1** (100 mg, 0.17 mmol) in THF (10 mL). Then the reaction mixture was stirred for a further 2 h before quenching with saturated NH$_4$Cl solution (10 mL). The mixture was extracted with dichloromethane (20 mL×3). Then the combined organic extracts were dried over MgSO$_4$. After evaporation of solvent under reduced pressure, the residue was dissolved in THF (5 mL) and a solution of 10% aqueous HCl (5 mL) saturated with $SnCl_2$ was added carefully until the flask content no longer bubbled on addition of the $SnCl_2$ solution. The solution was then heated to reflux for 1 h before being allowed to cool. The mixture was filtered through a short pad of silica gel eluting with hexanes and the solvent was removed under reduced pressure. The resulting crude product was purified by column chromatography on silica gel (20 g, hexanes) to afford **7** (122 mg, 76%) as a purple-red solid: mp 326 °C (decomp.); ^{1}H NMR (CDCl$_3$) δ 0.40 (s, 36H), 7.51–7.60 (m, 6H), 7.95 (dd, J=1.2, 8.0 Hz, 4H), 8.34 (s, 4H), 9.22 (s, 4H); ^{13}C NMR (CD$_2$Cl$_2$) δ 1.17, 124.9, 127.3, 128.3, 128.7, 129.4, 131.3, 136.2, 137.1, 139.1, 140.4; MS m/z 718 (M$^+$), HRMS (ESI) Calcd for $C_{46}H_{54}Si_4$ (M$^+$): 718.3297. Found: 718.3313.

3.1.2.2. 6,13-Di(p-tolyl)-2,3,9,10-tetrakis(trimethylsilyl)pentacene (8). This was prepared from 4-bromotoluene (0.42 mL, 3.4 mmol), ^{n}BuLi (2.1 mL, 3.4 mmol), **1** (100 mg, 0.17 mmol), and 10% HCl (5 mL) saturated with $SnCl_2$ in THF (10 mL) in the same manner as described above, yielding **8** (101 mg, 80%) as a purple-red solid: mp 320 °C (decomp.); ^{1}H NMR (CD$_2$Cl$_2$) δ 0.40 (s, 36H), 2.63 (s, 6H), 7.53 (d, J=4.2 Hz, 8H), 8.04 (s, 4H), 8.29 (s,

4H); ^{13}C NMR (CD$_2$Cl$_2$) δ 1.2, 20.9, 125.0, 127.6, 128.3, 129.0, 129.4, 131.2, 136.0, 136.2, 137.1, 140.3; MS m/z 746 (M$^+$), HRMS (ESI) Calcd for C$_{48}$H$_{58}$Si$_4$ (M$^+$): 746.3610. Found: 746.3614.

3.1.2.3. 6,13-Di(*p*-anisyl)-2,3,9,10-tetrakis(trimethylsilyl)pentacene (9). This was prepared from 4-bromoanisole (0.42 mL, 3.4 mmol), ^{n}BuLi (2.1 mL, 3.4 mmol), **1** (100 mg, 0.17 mmol), and 10% HCl (5 mL) saturated with SnCl$_2$ in THF (10 mL) in the same manner as described above, yielding **9** (86 mg, 65%) as a purple-red solid: mp 326 °C (decomp.); ^{1}H NMR (CD$_2$Cl$_2$) δ 0.30 (s, 36H), 4.03 (s, 6H), 7.27 (d, J=8.4 Hz, 4H), 7.53 (d, J=8.4 Hz, 4H), 8.04 (s, 4H), 8.28 (s, 4H); ^{13}C NMR (CD$_2$Cl$_2$) δ 2.2, 56.0, 114.7, 126.0, 127.7, 130.1, 130.4, 132.1, 133.3, 137.2, 141.3, 159.9; MS m/z 778 (M$^+$), HRMS (ESI) Calcd for C$_{48}$H$_{58}$O$_2$Si$_4$ (M$^+$): 778.3508. Found: 778.3515. Anal. Calcd for: C$_{48}$H$_{58}$O$_2$Si$_4$: C, 73.98; H, 7.50. Found: C, 73.57; H, 7.67.

3.1.2.4. 6,13-Di(*p*-cyanophenyl)-2,3,9,10-tetrakis(trimethylsilyl)pentacene (10). This was prepared from 4-bromobenzonitrile (619 mg, 3.4 mmol), ^{n}BuLi (2.1 mL, 3.4 mmol), **1** (100 mg, 0.17 mmol), and 10% HCl (5 mL) saturated with SnCl$_2$ in THF (10 mL) in the same manner as described above, yielding **10** (109 mg, 84%) as a purple-red solid: mp 320 °C (decomp.); ^{1}H NMR (CD$_2$Cl$_2$) δ 0.39 (s, 36H), 7.75 (d, J=8.1 Hz, 4H), 8.05 (d, J=7.8 Hz, 4H), 8.11 (s, 4H), 8.03 (s, 4H); ^{13}C NMR (CD$_2$Cl$_2$) δ 1.1, 111.6, 118.6, 124.3, 128.1, 129.8, 132.1, 132.4, 135.5, 135.9, 141.4, 144.1; MS m/z 768 (M$^+$), HRMS (ESI) Calcd for C$_{48}$H$_{52}$N$_2$Si$_4$ (M$^+$): 768.3202. Found: 768.3189.

3.1.2.5. 6,13-Di(1,3-dimethylphenyl)-2,3,9,10-tetrakis(trimethylsilyl)pentacene (11). This was prepared from 2-bromo-1,3-dimethylbenzene (0.45 mL, 3.4 mmol), ^{n}BuLi (2.1 mL, 3.4 mmol), **1** (100 mg, 0.17 mmol), and 10% HCl (5 mL) saturated with SnCl$_2$ in THF (10 mL) in the same manner as described above, yielding **11** (92 mg, 70%) as a purple-red solid: mp 328 °C (decomp.); ^{1}H NMR (CD$_2$Cl$_2$) δ 0.40 (s, 36H), 1.80 (s, 12H), 7.42 (d, J=7.8 Hz, 4H), 7.49–7.54 (m, 2H), 8.03 (s, 4H), 8.07 (s, 4H); ^{13}C NMR (CD$_2$Cl$_2$) δ 1.2, 19.4, 124.2, 127.4, 127.5, 128.2, 130.0, 135.6, 136.2, 137.6, 137.9, 140.3; MS m/z 774 (M$^+$), HRMS (ESI) Calcd for C$_{50}$H$_{62}$Si$_4$ (M$^+$): 774.3923. Found: 774.3915. Anal. Calcd for: C$_{50}$H$_{62}$Si$_4$: C, 77.45; H, 8.06. Found: C, 77.48; H, 8.19.

3.1.2.6. 6,13-Dithienyl-2,3,9,10-tetrakis(trimethylsilyl)pentacene (12). This was prepared from thiophene (0.27 mL, 3.4 mmol), ^{n}BuLi (2.1 mL, 3.4 mmol), **1** (100 mg, 0.17 mmol), and 10% HCl (5 mL) saturated with SnCl$_2$ in THF (10 mL) in the same manner as described above, yielding **12** (94 mg, 76%) as a purple-red solid: mp 368 °C (decomp.); ^{1}H NMR (CD$_2$Cl$_2$) δ 0.42 (s, 36H), 7.42 (d, J=1.8 Hz, 2H), 7.48 (dd, J=3.3, 5.1 Hz, 2H), 7.80 (d, J=5.1 Hz, 4H), 8.11 (s, 4H), 8.44 (s, 4H); ^{13}C NMR (CD$_2$Cl$_2$) δ 1.2, 124.7, 125.0, 126.8, 127.1, 129.7, 129.8, 130.1, 136.1, 138.8, 141.0; MS m/z 730 (M$^+$), HRMS (ESI) Calcd for C$_{42}$H$_{50}$S$_2$Si$_4$ (M$^+$): 730.2426. Found: 730.2416.

3.1.2.7. 6,13-Di(5-trimethylsilylthien-2-yl)-2,3,9,10-tetrakis(trimethylsilyl)pentacene (13). This was prepared from trimethyl-2-thienylsilane (0.56 mL, 3.4 mmol), ^{n}BuLi (2.1 mL, 3.4 mmol), **1** (100 mg, 0.17 mmol), and 10% HCl (5 mL) saturated with SnCl$_2$ in THF (10 mL) in the same manner as described above, yielding **13** (119 mg, 80%) as a purple-red solid: mp 368 °C (decomp.); ^{1}H NMR (CDCl$_3$) δ 0.48 (s, 36H), 0.56 (s, 18H), 7.52 (d, J=3.3 Hz, 2H), 7.68 (d, J=3.3 Hz, 2H), 8.14 (s, 4H), 8.47 (s, 4H); ^{13}C NMR (CDCl$_3$) δ 0.3, 1.9, 125.3, 127.2, 127.5, 130.2, 130.6, 131.4, 134.3, 136.7, 141.0, 144.9; MS m/z 874 (M$^+$), HRMS (ESI) Calcd for C$_{48}$H$_{66}$S$_2$Si$_6$ (M$^+$): 874.3216. Found: 874.3207.

3.1.2.8. 6,13-Bis(2′-[*tert*-butyldimethylsilyl]-1′,2′-carboranyl-*p*-methylphenyl)-2,3,9,10-tetrakis(trimethylsilyl)pentacene (15). To a solution of 2-(*tert*-butyldimethylsilyl)-1,2-carboranyl-*p*-methylbenzobromide[31] (284 mg, 0.68 mmol) in THF (10 mL) at −50 °C was added ^{n}BuLi (0.48 mL, 0.77 mmol) dropwise. After stirring for 1 h at −50 °C, the aryllithium was transferred dropwise to the solution of **1** (100 mg, 0.17 mmol) in THF (10 mL). Then the reaction mixture was stirred for a further 2 h before quenching with saturated NH$_4$Cl solution (10 mL). The mixture was extracted with dichloromethane (20 mL×3). Then the combined organic extracts were dried over MgSO$_4$. After evaporation of solvent under reduced pressure, the residue was dissolved in THF (5 mL) and a solution of 10% aqueous HCl (5 mL) saturated with SnCl$_2$ was added carefully until the flask content no longer bubbled on addition of the SnCl$_2$ solution. The solution was then heated to reflux for 1 h before being allowed to cool. The mixture was filtered through a short pad of silica gel eluting with hexanes and the solvent was removed under reduced pressure. The resulting crude product was purified by column chromatography on silica gel (20 g, hexanes) to afford **15** (23 mg, 11%) as a purple-red solid: mp 320 °C (decomp.); ^{1}H NMR (CD$_2$Cl$_2$) δ 0.34 (s, 36H), 0.50 (s, 12H), 1.19 (s, 18H), 3.75 (s, 4H), 7.51–7.59 (m, 8H), 7.96 (s, 4H), 8.12 (s, 4H); ^{11}B NMR (CD$_2$Cl$_2$) δ 0.31 (s, 2B), −4.03 (s, 2B), −7.28 (s, 6B), −9.73 (s, 10B); ^{13}C NMR (CD$_2$Cl$_2$) δ −2.5, 1.3, 20.3, 27.4, 43.3, 75.4, 81.4, 125.0, 128.7, 129.6, 130.0, 131.7, 135.4, 136.3, 139.2, 140.8; MS m/z 1260 ([M+2]$^+$), HRMS (ESI) Calcd for C$_{64}$H$_{106}$Si$_6$^{11}B$_{16}$^{10}B$_4$ (M$^+$): 1258.8911. Found: 1258.8920.

3.1.2.9. 6-Chloro-2,3,9,10-tetrakis(trimethylsilyl)pentacene (16). To a suspension of LiAlH$_4$ (100 mg, 2.97 mmol) in THF (10 mL), **1** (100 mg, 0.17 mmol) in THF (5 mL) was added under N$_2$ at 0 °C. After stirring for 15 min, crude ethyl acetate (20 mL) was added dropwise to decompose the excess LiAlH$_4$ before pouring the mixture into water (10 mL). The resulting mixture was extracted with ethyl acetate (10 mL×3). The combined organic extracts were dried over MgSO$_4$ and concentrated under reduced pressure. The orange residue was purified by column chromatography on silica gel (20 g, hexanes/ethyl acetate=5:1) to provide an orange solid, which was then used without further purification.

To the solution of DMAP (2 mg, 0.02 mmol) and triethylamine (0.14 mL, 1.0 mmol) in degassed CH$_2$Cl$_2$ (10 mL), the degassed orange residue obtained above was added under N$_2$. After stirring for 30 min, methanesulfonyl chloride (0.09 mL, 0.68 mmol) was added under N$_2$ via a syringe.

After stirring for a further 30 min, the solvent was evaporated under vacuum. The solid residue was then transferred to the silica gel column with rigorous exclusion of air (10 g, hexanes). Purple-red eluent was collected under N_2 to afford **16** (46 mg, 46%) as a purple-red solid after evaporation: mp 320 °C (decomp.); ^{1}H NMR (CDCl$_3$) δ 0.52 (s, 18H), 0.53 (s, 18H), 8.25 (s, 2H), 8.33 (s, 2H), 8.61 (s, 2H), 8.92 (s, 1H), 9.05 (s, 2H); ^{13}C NMR (CDCl$_3$) δ 1.9, 123.4, 126.7, 126.9, 127.7, 128.4, 130.4, 130.6, 131.2, 136.1, 137.0, 141.5, 141.7; MS m/z 600 (M$^+$), HRMS (FAB) Calcd for C$_{34}$H$_{45}$ClSi$_4$ (M$^+$): 600.2292. Found: 600.2299.

3.1.3. General procedure for the preparation of Diels–Alder adducts 17–21.

3.1.3.1. 2,3,9,10-Tetrakis(trimethylsilyl)-6-chloro-13-hydro-6,13-ethenopentacene-15,16-dicarboxylate (17). A solution of **16** (25 mg, 0.042 mmol) in CH$_2$Cl$_2$ (5 mL) was added to a solution of DMAD (0.01 mL, 0.09 mmol) in CH$_2$Cl$_2$ (5 mL) dropwise at room temperature under N_2. After stirring for 2 days, the color of the reaction mixture changed from purple-red to pale yellow and the solvent was removed under reduced pressure. The resulting crude product was purified by chromatography on silica gel (10 g, hexanes: ethyl acetate=10:1) to afford **17** (11 mg, 36%) as a colorless powder: mp 150 °C; ^{1}H NMR (CDCl$_3$) δ 0.39 (s, 18H), 0.40 (s, 18H), 3.78 (s, 3H), 3.85 (s, 3H), 5.87 (s, 1H), 7.82 (s, 2H), 8.04 (s, 2H), 8.10 (s, 4H); ^{13}C NMR (CDCl$_3$) δ 1.9, 48.6, 52.6, 52.8, 72.5, 121.2, 121.9, 130.3, 130.9, 134.8, 135.8, 138.4, 138.7, 139.0, 143.0, 143.5, 152.3, 163.0, 165.1; MS m/z 765 ([M+Na]$^+$), HRMS (ESI) Calcd for C$_{40}$H$_{51}$O$_4$ClSi$_4$ ([M+Na]$^+$): 765.2445. Found: 765.2434.

3.1.3.2. 2,3,9,10-Tetrakis(trimethylsilyl)-6-chloro-13-hydro-6,13-ethanopentacene-17-phenyl-17H-pyrrole-16,18-dione (18). A solution of **16** (25 mg, 0.042 mmol) in CH$_2$Cl$_2$ (5 mL) was added to a solution of N-phenyl maleimide (7.5 mg, 0.042 mmol) in CH$_2$Cl$_2$ (5 mL) dropwise at room temperature under N_2. After stirring for 12 h, the color of the reaction mixture changed from purple-red to pale yellow, and the solvent was removed under reduced pressure. The resulting crude product was purified by chromatography on silica gel (10 g, hexanes/ethyl acetate=10:1) to afford **18** (27 mg, 86%) as a colorless powder: mp 165 °C; ^{1}H NMR (CDCl$_3$) δ 0.41 (s, 9H), 0.42 (s, 9H), 0.43 (s, 9H), 0.44 (s, 9H), 3.61 (d, J=1.5 Hz, 2H), 5.13 (s, 1H), 6.32 (d, J=7.2 Hz, 2H), 7.13 (m, 3H), 7.79 (s, 1H), 7.85 (s, 1H), 8.08 (s, 1H), 8.14 (s, 1H), 8.15 (s, 1H), 8.18 (s, 1H), 8.22 (s, 1H), 8.30 (s, 1H); ^{13}C NMR (CDCl$_3$) δ 1.9, 45.2, 48.5, 52.8, 70.4, 122.2, 122.6, 123.6, 126.2, 128.7, 128.9, 131.0, 131.2, 131.6, 134.1, 134.9, 135.6, 135.9, 136.0, 137.0, 138.5, 143.2, 143.6, 143.8, 172.5, 174.8; MS m/z 774 ([MH]$^+$), HRMS (FAB) Calcd for C$_{44}$H$_{52}$NO$_2$ClSi$_4$ ([MH]$^+$): 774.2836. Found: 774.2832.

3.1.3.3. 2,3,9,10-Tetrakis(trimethylsilyl)-6-chloro-13-hydro-13,15,16,17,18-pentahydro-6,13(1′,2′)-benzeno-pentacene-15,18-dione (19). This was prepared from **16** (25 mg, 0.042 mmol) and *p*-benzoquinone (4.5 mg, 0.042 mmol) in CH$_2$Cl$_2$ (5 mL) in the same manner as described above, yielding **19** (23 mg, 80%) as a pale-yellow solid: mp 190 °C; ^{1}H NMR (CDCl$_3$) δ 0.41 (s, 9H), 0.42 (s, 9H), 0.427 (s, 9H), 0.432 (s, 9H), 3.30 (d, J=9.6 Hz, 1H), 3.39 (dd, J=3.0, 9.3 Hz, 1H), 4.97 (d, J=3.0 Hz, 1H), 6.07

(d, J=10.2 Hz, 1H), 6.22 (d, J=10.2 Hz, 1H), 7.65 (s, 1H), 7.85 (s, 1H), 8.05 (s, 1H), 8.06 (s, 1H), 8.12 (s, 1H), 8.13 (s, 1H), 8.20 (s, 1H), 8.24 (s, 1H); ^{13}C NMR (CDCl$_3$) δ 1.9, 48.8, 51.2, 56.4, 71.6, 121.7, 122.1, 122.7, 123.1, 131.1, 131.2, 131.5, 131.7, 134.9, 135.0, 135.5, 135.9, 136.0, 136.2, 136.7, 139.1, 139.2, 141.4, 143.1, 143.2, 143.58, 143.6, 194.3, 197.3; MS m/z 731 ([M+Na]$^+$), HRMS (ESI) Calcd for C$_{40}$H$_{49}$O$_2$ClSi$_4$ ([M+Na]$^+$): 731.2390. Found: 731.2381.

3.1.3.4. 2,3,9,10-Tetrakis(trimethylsilyl)-6-chloro-13,16,17-trihydro-6,13(1′,2′)-naphthalenopentacene-15,18-dione (20). This was prepared from **16** (25 mg, 0.042 mmol) and naphthaquinone (6 mg, 0.042 mmol) in CH$_2$Cl$_2$ (10 mL) in the same manner as described above, yielding **20** (15 mg, 48%) as a pale-yellow solid: mp 191 °C; ^{1}H NMR (CDCl$_3$) δ 0.35 (s, 9H), 0.36 (s, 9H), 0.43 (s, 18H), 3.56 (d, J=9.6 Hz, 1H), 3.65 (dd, J=3.0, 9.45 Hz, 1H), 5.12 (d, J=3.0 Hz, 1H), 7.15–7.21 (m, 1H), 7.28–7.33 (m, 1H), 7.46 (d, J=7.5 Hz, 1H), 7.50 (s, 1H), 7.60 (d, J=7.5 Hz, 1H), 7.77 (s, 1H), 7.86 (s, 1H), 7.87 (s, 1H), 7.88 (s, 1H), 8.13 (s, 1H), 8.20 (s, 1H), 8.24 (s, 1H); ^{13}C NMR (CDCl$_3$) δ 1.9, 49.0, 51.7, 57.4, 71.8, 121.4, 122.1, 122.8, 123.1, 125.7, 125.9, 130.8, 131.2, 131.6, 133.2, 133.8, 134.6, 134.7, 134.9, 135.4, 135.6, 136.0, 136.1, 136.6, 137.0, 139.8, 142.5, 142.9, 143.0, 143.4, 194.1, 196.3; MS m/z 781 ([M+Na]$^+$), HRMS (ESI) Calcd for C$_{44}$H$_{51}$O$_2$ClSi$_4$ ([M+Na]$^+$): 781.2547. Found: 781.2551.

3.1.3.5. 2,3,9,10-Tetrakis(trimethylsilyl)-6-chloro-13,16,17-trihydro-6,13(1′,2′)-anthracenopentacene-15,18-dione (21). This was prepared from **16** (25 mg, 0.042 mmol) and anthraquinone (9 mg, 0.042 mmol) in CH$_2$Cl$_2$ (10 mL) in the same manner as described above, yielding **21** (14 mg, 43%) as an orange solid: mp 198 °C; ^{1}H NMR (CDCl$_3$) δ 0.23 (s, 9H), 0.33 (s, 9H), 0.44 (s, 18H), 3.59 (d, J=9.6 Hz, 1H), 3.71 (dd, J=3.3, 9.3 Hz, 1H), 5.15 (d, J=3.3 Hz, 1H), 7.35–7.45 (m, 2H), 7.47 (s, 1H), 7.52 (d, J=8.4 Hz, 1H), 7.55 (s, 1H), 7.63 (s, 1H), 7.76 (d, J=8.4 Hz, 1H), 7.79 (s, 1H), 7.82 (s, 1H), 7.91 (s, 1H), 8.06 (s, 1H), 8.16 (s, 1H), 8.22 (s, 1H), 8.27 (s, 1H); ^{13}C NMR (CDCl$_3$) δ 1.0, 1.8, 1.9, 49.3, 52.2, 58.0, 71.9, 121.4, 122.2, 123.1, 123.2, 127.0, 127.5, 128.6, 128.9, 129.1, 129.3, 130.6, 131.0, 131.2, 131.7, 132.8, 134.2, 134.4, 134.6, 134.9, 135.1, 135.7, 135.9, 136.0, 136.8, 139.8, 142.2, 142.8, 142.9, 143.4, 194.5, 196.8; MS m/z 831 ([M+Na]$^+$), HRMS (ESI) Calcd for C$_{48}$H$_{53}$O$_2$ClSi$_4$ ([M+Na]$^+$): 831.2703. Found: 831.2713.

References and notes

1. Chan, S. H.; Lee, H. K.; Wang, Y. M.; Fu, N. Y.; Chen, X. M.; Cai, Z.; Wong, H. N. C. *Chem. Commun.* **2005**, 66.

2. Takahashi, T.; Kitamura, M.; Shen, B.; Nakajima, K. *J. Am. Chem. Soc.* **2000**, *122*, 12876.

3. Halik, M.; Klauk, H.; Zschieschang, U.; Schmid, G.; Dehm, C.; Schutz, M.; Maisch, S.; Effenberger, F.; Brunnbauer, M.; Stellaccl, F. *Nature* **2004**, *431*, 963.

4. Maliakal, A.; Raghavachari, K.; Katz, H.; Chandross, E.; Siegrist, T. *Chem. Mater.* **2004**, *16*, 4980.

5. Coppo, P.; Yeates, S. G. *Adv. Mater.* **2005**, *17*, 3001.

6. Miao, Q.; Chi, X.; Xiao, S.; Zeis, R.; Lefenfeld, M.; Siegrist, T.; Steigenwald, M. L.; Nuckolls, C. *J. Am. Chem. Soc.* **2006**, *128*, 1340.

7. Tulevski, G. S.; Miao, Q.; Afzali, A.; Graham, T. O.; Kagan, C. R.; Nuckolls, C. *J. Am. Chem. Soc.* **2006**, *128*, 1788.

8. Vets, N.; Smet, M.; Dehaen, W. *Synlett* **2005**, 217.

9. Vets, N.; Diliën, H.; Toppet, S.; Dehaen, W. *Synlett* **2006**, 1359.

10. Wolak, M. A.; Jang, B. B.; Palilis, L. C.; Kafafi, Z. H. *J. Phys. Chem. B* **2004**, *108*, 5492.

11. Jiang, J.; Kaafarani, B. R.; Neckers, D. C. *J. Org. Chem.* **2006**, *71*, 2155.

12. Anthony, J. E.; Brooks, J. S.; Eaton, D. L.; Parkin, S. R. *J. Am. Chem. Soc.* **2001**, *123*, 9482.

13. Payne, M. M.; Parkin, S. R.; Anthony, J. E.; Kuo, C.; Jackson, T. N. *J. Am. Chem. Soc.* **2005**, *127*, 4986.

14. Sheraw, C. D.; Jackson, T. N.; Eaton, D. L.; Anthony, J. E. *Adv. Mater.* **2003**, *15*, 2009.

15. Payne, M. M.; Delcamp, J. H.; Parkin, S. R.; Anthony, J. E. *Org. Lett.* **2004**, *6*, 1609.

16. Anthony, J. E.; Eaton, D. L.; Parkin, S. R. *Org. Lett.* **2002**, *4*, 15.

17. Reichwagen, J.; Hopf, H.; Desvergne, J.; Guerzo, A. D.; Bouas-Laurent, H. *Synthesis* **2005**, 3505.

18. Chan, S. H.; Yick, C. Y.; Wong, H. N. C. *Tetrahedron* **2002**, *58*, 9413.

19. X-ray data for **9** (data have been deposited with the Cambridge Crystallographic Data Centre as supplementary publication no. CCDC 638195): Triclinic, space group *P*-1, a=9.4084 (11) Å, b=11.7419 (14) Å, c=13.5170 (16) Å, α=98.537 (2)°, β=107.468 (2)°, γ=112.039 (2)°, V=1261.4 (3) Å^3; Z=1; D_c=1.249 Kg/m^3; T=180 K; final R indices (obsd): R_1=0.0448, ωR_2=0.1337; R indices (all): R_1=0.0552, ωR_2=0.1395.

20. Holmes, D.; Kumaraswamy, S.; Matzger, A. J.; Vollhardt, K. P. C. *Chem.—Eur. J.* **1999**, *5*, 3399.

21. Mattheus, C. C.; Dros, A. B.; Baas, J.; Meetsma, A.; de Boer, J. L.; Palstra, T. T. M. *Acta Crystallogr.* **2001**, *C57*, 939.

22. Bendikov, M.; Duong, H. M.; Starkey, K.; Houk, K. N.; Carter, E. A.; Wudl, F. *J. Am. Chem. Soc.* **2004**, *126*, 7416.

23. Houk, K. N.; Lee, P. S.; Nendel, M. *J. Org. Chem.* **2001**, *66*, 5517.

24. Ruiz-Morales, Y. *J. Phys. Chem. A* **2002**, *106*, 11283.

25. Nijegorodov, N.; Ramachandran, V.; Winkoun, D. P. *Spectrochim. Acta, Part A* **1997**, *53*, 1813.

26. Schleyer, P. v. R.; Maerker, C.; Dransfeld, A.; Jiao, H.; Hommes, N. J. R. E. *J. Am. Chem. Soc.* **1996**, *118*, 6317.

27. Chen, Z.; Wannere, C. S.; Corminboeuf, C.; Puchta, R.; Schleyer, P. v. R. *Chem. Rev.* **2005**, *105*, 3842.

28. Schleyer, P. v. R.; Manoharan, M.; Jiao, H.; Stahl, F. *Org. Lett.* **2001**, *3*, 3643.

29. X-ray data for **15** (data have been deposited with the Cambridge Crystallographic Data Centre as supplementary publication no. CCDC 638196): triclinic, space group *P*-1, a=14.7251 (17) Å, b=23.273 (2) Å, c=13.2470 (14) Å, α=90.00°, β=108.879 (2)°, γ=90.00°, V=4295.4 (8) Å^3; Z=2; D_c=1.249 Kg/m^3; T=293 (2) K; final R indices [I>2σ(I)]: R_1=0.0856, ωR_2=0.2117; R indices (all data): R_1=0.2195, ωR_2=0.3148.

30. X-ray data for **16** (data have been deposited with the Cambridge Crystallographic Data Centre as supplementary publication no. CCDC 638197): triclinic, space group *P*-1, a=9.584 (2) Å, b=12.072 (3) Å, c=15.685 (4) Å, α=89.654 (6)°, β=78.430 (5)°, γ=80.523 (5)°, V=1752.9 (7) Å^3; Z=2; D_c=1.140 Kg/m^3; T=293 (2) K; final R indices [I>2σ(I)]: R_1=0.0565, ωR_2=0.1576; R indices (all data): R_1=0.0936, ωR_2=0.1912.

31. 2-(*tert*-Butyldimethylsilyl)-1,2-carboranyl-*p*-methylbenzobromide (**15**) was easily prepared from *o*-carborane and *p*-bromobenzyl bromide followed the step (Gomez, F. A.; Hawthorne, M. F. *J. Org. Chem.* **1992**, *57*, 1384). ^{1}H NMR (CDCl$_3$) δ 0.42 (s, 6H), 1.13 (s, 9H), 3.42 (s, 2H), 7.02 (d, *J*=8.4 Hz), 7.46 (d, *J*=8.4 Hz); ^{13}C NMR (CDCl$_3$) δ −2.2, 20.5, 27.7, 42.8, 75.1, 80.4, 122.2, 131.5, 131.8, 134.7; MS *m/z* 427 (M$^+$), HRMS (ESI) Calcd for C$_{15}$H$_{31}$Si$_6$^{11}B$_8$^{10}B$_2$Br (M+): 425.2298. Found: 425.2319.